Wide Broadband ASE Source based on Thulium-doped Fibre for 2 μm Wavelength Region

M. A. Khamis and K. Ennser
College of Engineering, Swansea University, Swansea, U.K.

Keywords: Thulium-doped Fibre, Amplified Spontaneous Emission, Silica Glass Material, Numerical Modelling.

Abstract: This paper investigates the generation of the amplified spontaneous emission (ASE) from thulium-doped silica fibre pumped at 1570 nm. The developed model provides the ASE spectral power at short and long wavelength bands by using two different thulium doped fibre types with optimized fibre length. Shorter wavelengths in the emission band can be accessed with a short thulium fibre, whereas longer wavelengths can be obtained using a long thulium fibre. Our findings reveal that, in contrast to a 100 nm (1800nm-1900nm) and 70 nm (1900nm-1970nm) broadband source at short and long wavelength bands, a broader spectrum source can be achieved at about 170 nm (1800nm-1970nm) by a combined of the two ASE spectra via a wideband 50:50 coupler. As a result, the proposed ASE source configuration doubles the bandwidth of the conventional single fibre based light source.

1 INTRODUCTION

Over the last few years, broadband sources near 2 μm have attracted the attention of many researchers. Hu et al. (2015) point out a broadband source at 2 μm have many useful characteristics, including high output power, high light brightness, good beam quality, compact structure and excellent spatial coherence. These characteristics make broadband sources at 2 μm suitable for use in a number of significant applications, such as remote sensing (Li et al., 2014), gas sensing (Hsu et al., 2008), medical surgery (Morse et al. 1995), materials processing (Jackson Sabella and Lancaster, 2007) and atmospheric lidar measurement (Sugimoto et al.,1990). In addition, according to Halder et al. (2012) and Cheung et al. (2015), high power and wideband sources are required in optical coherence tomography and fibre optic gyroscopes.

One effective way to generate this broadband source is by using the process of amplified spontaneous emission between $^3F_4$-$^3H_6$ transition in thulium-doped fibre. High broadband source efficiency can be obtained via diode pumping on the transition $^3H_6 \rightarrow {}^3H_4$ in combination with high concentration of thulium-doped silica fibre in order to take into account the cross-relaxation process (Oh, 1994; Shen et al., 2008). Alternatively, the need for high doping concentrations can be avoided by using an in-band pumping scheme, which directly excites the upper laser level on the transition $^3H_6 \rightarrow {}^3F_4$. Nevertheless, Tsang et al. (2005) explain that high efficiencies can be achieved because of the much lower quanta defect associated with this pumping scheme. However, in spite of the progress in the performance of thulium broadband sources the efficiency and bandwidth are still below those routinely provided from conventional thulium fibre laser oscillators.

To better optimize the broadband source performance near 2 μm. It is necessary to develop a theoretical modeling and perform simulations. There are relatively few theoretical studies on ASE sources based on thulium-doped fibre (TDF) (Gorjan et al., 2012; Yu et al., 2010). On the other hand, various experimental configurations for broadening the spectral bandwidth of ASE source have been presented in the literature. Broader bandwidths up to 72 nm have been demonstrated using Tm: Ho-doped silica fibre (Tsang et al., 2005). Up to 100 nm of broadband spectra has been achieved using single end operation (Shen et al., 2008). However, these configurations have limited spectra bandwidth. This paper proposes a new thulium ASE configuration that doubles the bandwidth of the conventional configuration.

In this paper, a broadening ASE source can be generated from combining the ASE output source of

Khamis M. and Ennser K.
Wide Broadband ASE Source based on Thulium-doped Fibre for 2 Îijm Wavelength Region.
DOI: 10.5220/0006101801410146
In *Proceedings of the 5th International Conference on Photonics, Optics and Laser Technology (PHOTOPTICS 2017)*, pages 141-146
ISBN: 978-989-758-223-3

two different TDFs as shown in fig.(1). The first fibre TDF_1 is a commercial thulium fibre (TmDF200 from OFS) with short fibre length. Agger and Povlsen (2006) demonstrated that the center emission spectrum of this fibre is at the wavelength 1800 nm. The second fibre TDF_2 is a commercial thulium fibre (SM-TSF-9/125 from Nufern) with long fibre length. Jackson (2009) shows that this fibre produces an emission spectrum with 1900 nm center wavelength. Long TDF leads to shift the output spectrum to ward long wavelength bands (Li et al. 2013). Thus, TDF_1 generated ASE1 source with short wavelength bands which is centered at 1840nm and TDF_2 produced ASE2 source with long wavelength bands which is centered at 1950nm. The two ASE sources were combined together into a single ASE source via wideband 50:50 coupler. This type of coupler is already applied to design a widely tunable thulium laser (Stevens and Legg 2015). Notes that in our simulation, we choose couplers and combiners have flatting coupling response over the wavelengths range in order to allow broadband ASE source.

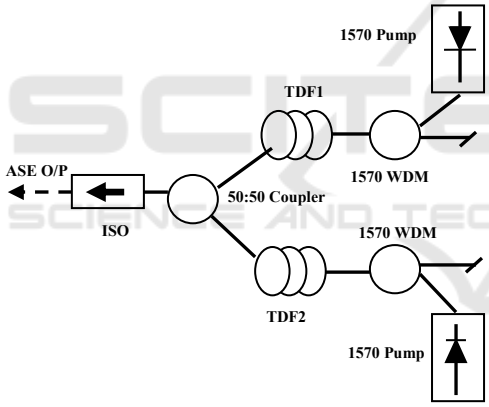

Figure 1: A schematic diagram of proposed ASE source. ISO is an optical isolator at 2μm, ASE o/p is the combined ASE sources of TDF_1 and TDF_2 ASE output. Note that all fibre ends are angle polished.

2 NUMERICAL MODEL OF ASE

A theoretical model of ASE generation are presented. The investigation into ASE spectral power is achieved by solving the rate and propagation equations. The model takes into account the wavelength-dependent absorption and emission cross-sections. Based on Jackson and King (1999) and including ASE, the rate equations of thulium energy levels are established as follows:

$$\frac{dN_2}{dt} = w_{p12}N_1(z,t) - w_{p21}N_2(z,t) - \frac{N_2}{\tau_2} - w_{s21}N_2(z,t) + w_{s12}N_1(z,t) \quad (1)$$

$$N_1(z,t) = N_T - N_2(z,t) \quad (2)$$

Here N_T is the Tm^{3+} concentration and set to be a constant. τ_2 is the spontaneous lifetime of the $^3F_4$, level N_1 and N_2 are the population densities of the $^3H_6$ and $^3F_4$ levels, respectively, w_{p12} is the pumping rate from $^3H_6$ to $^3F_4$ and w_{p21} represents the de-excitation of the $^3F_4$ level; w_{s21} is the stimulated emission rate from $^3F_4$ to $^3H_6$, and w_{s12} is the stimulated absorption rate from $^3H_6$ to $^3F_4$. The expressions of w_{p12}, w_{p21}, w_{s21} and w_{s12} can be obtained from:

$$w_{p12} = \frac{\lambda_p \Gamma_p}{hcA_{core}} \sigma_a(\lambda_p)(p_p^-(z) + p_p^+(z)) \quad (3)$$

$$w_{p21} = \frac{\lambda_p \Gamma_p}{hcA_{core}} \sigma_e(\lambda_p)(p_p^-(z) + p_p^+(z)) \quad (4)$$

$$w_{s12} = \frac{\lambda_s \Gamma_s}{hcA_{core}} \sigma_a(\lambda_s)[ASE_f(z) + ASE_b(z)] \quad (5)$$

$$w_{s21} = \frac{\lambda_s \Gamma_s}{hcA_{core}} \sigma_e(\lambda_s)[ASE_f(z) + ASE_b(z)] \quad (6)$$

Here λ_p is the wavelength of the pump light and λ_s is the signal light in vacuum; h is the Planck constant; c is the light speed in vacuum; A_{core} is the cross-section area of the fibre core; $\sigma_a(\lambda_p)$ and $\sigma_a(\lambda_s)$ are the absorption cross-sections of the pump light and the signal light, respectively; $\sigma_e(\lambda_p)$ and $\sigma_e(\lambda_s)$ are the emission cross-sections of the pump light and the signal light, respectively; $P^{\pm}(z)$ is the pump (corresponding to forward and backward) at position z; and $ASE^+(z)$ and $ASE^-(z)$ are the forward and backward amplified spontaneous emission powers at position z; Γ_p and Γ_s are the confinement factors for the pump and the signal, respectively which are given by Eq. 7 (Whitley and Wyatt, 1993).

$$\Gamma(\lambda) = 1 - \exp\left(-\frac{2a^2}{w^2}\right) \quad (7)$$

Where w is the mode-width parameter of the fibre and a is the radius of the fibre. The normalized frequency V of the fibre is given by:

$$V = \frac{2\pi a.NA}{\lambda} \quad (8)$$

As V> 1.5 the mode-width parameter *w* of a step-index fibre can be determined by the normalized frequency *V* of the fibre as:

$$\frac{w}{a} = 0.632 + 1.478\ V^{-3/2} + 4.76\ V^{-6} \quad (9)$$

Meanwhile, the pump power distribution along the fibre length can be expressed by the following propagation equation:

$$\frac{dp_p^{\pm}}{dz} = \pm p_p^{\pm}(z)[\ \Gamma_p(\sigma_e(\lambda_p)N_2(z) - \sigma_a(\lambda_p)N_1(z)) - \alpha_p] \quad (10)$$

The positive sign in (10) relates to the forward direction and the negative sign to the reverse direction. The distribution of the ASE forward and backward powers along the fibre length can be established as follows (Hu et al., 2015; Yu et al., 2010):

$$\frac{dASE_f}{dz} = ASE_f(z)[\ \Gamma_s(\sigma_e(\lambda_s)N_2(z) - \sigma_a(\lambda_s)N_1(z)) - \alpha_s] + 2\sigma_e(\lambda_s)N_2(z)\frac{hc^2}{\lambda_s^3}\Delta\lambda \quad (11)$$

$$\frac{dASE_b}{dz} = -ASE_b(z)[\ \Gamma_s(\sigma_e(\lambda_s)N_2(z) - \sigma_a(\lambda_s)N_1(z)) - \alpha_s] - 2\sigma_e(\lambda_s)N_2(z)\frac{hc^2}{\lambda_s^3}\Delta\lambda \quad (12)$$

Where α_p and α_s are the intrinsic absorption at the pump and signal wavelength for the Thulium-doped fibre, respectively, $\Delta\lambda$ is the bandwidth of the amplified spontaneous emission (ASE) around 2µm.

3 RESULTS AND DISCUSSION

To solve the thulium rate equations for the ASE model in steady state condition, the time derivatives of eq. (1) to (2) for in-band pumping are set to zero. The fourth-order Runge-Kutta method is applied to solve the differential equations of the pump and the amplified spontaneous emission ASE signals. Table 1 and 2 summarizes all parameters values used in the numerical simulations of the TDF_1 (Agger and Povlsen 2006) and TDF_2 (Jackson 2009), respectively. Initially, the entire population is assumed to be at the ground level $^3H_6$ in the numerical calculations.

Table 1: Values of numerical parameters for TDF_1.

Symbol	Quantity	Value
N_T	Thulium concentration	8.4×10^{25} m^{-3}
τ_2	Lifetime of level $^3F_4$	650µs
λ_p	In-band pump wavelength	1570nm
$\sigma_a(\lambda_p)$	Laser absorption cross section at *1570nm.*	2.1×10^{-25} m^2
$\sigma_e(\lambda_p)$	Laser emission cross section at *1570nm.*	0
$\sigma_a(\lambda_s)$	Laser absorption cross section at signal wavelength	See (Agger and Povlsen, 2006)
$\sigma_e(\lambda_s)$	Laser emission cross section at signal wavelength	See (Agger and Povlsen, 2006)
NA	Numerical aperture	0.26
A	Area cross section of the core	3.1×10^{-11} m^{-2}
α_p	Intrinsic absorption at the pump wavelength	1.07×10^{-3} m^{-1}
α_s	Intrinsic absorption at the signal wavelength	1.15×10^{-2} m^{-1}

Table 2: Values of numerical parameters for TDF2.

Symbol	Quantity	Value
N_T	Thulium concentration	1.37×10^{25} m^{-3}
τ_2	Lifetime of level $^3F_4$	250µs
λ_p	In-band pump wavelength	1570nm
$\sigma_a(\lambda_p)$	Laser absorption cross section at *1570nm.*	2×10^{-25} m^2
$\sigma_e(\lambda_p)$	Laser emission cross section at *1570nm.*	0
$\sigma_a(\lambda_s)$	Laser absorption cross section at signal wavelength	See (Jackson 2009)
$\sigma_e(\lambda_s)$	Laser emission cross section at signal wavelength	See (Jackson 2009)
NA	Numerical aperture	0.15
A	Area cross section of the core	6.36×10^{-11} m^{-2}
α_p	Intrinsic absorption at the pump wavelength	1.07×10^{-3} m^{-1}
α_s	Intrinsic absorption at the signal wavelength	1.15×10^{-2} m^{-1}

Table 3 explains the initial conditions for the pump power and the ASE spectrum in forward and backward directions. The thulium-doped fibre with length L is divided into N segments along the z-direction. The solution is applied for the pump and the ASE power propagating in the first segment (segment 0) by using the initial conditions in Table 3. For the following segments (segment 1 to N-1), the power for the pump and the ASE at one end of a segment is applied as the input for the next segment. Relaxation method is used to solve the differential equations of the pump and the ASE powers (Emami 2011). Using the data of Table 1, 2 and the values of the emission and the absorption cross-section, we solve numerically the rate equations of the pump and ASE power distribution.

Table 3: Initial conditions.

Initial condition	Explanation
P^{+}_{p} (z=0) = Forward launched pumppower	Initial condition for 1558nm and 793nm pumps at z=0.
P^{-}_{p} (z=L) =Backward launched pump power	Initial condition for 1558nm and 793nm pumps at z=L.
P_s *(z=0)= seed power*	Initial condition for seed power at z=0.
ASE_f *(z=0)=0*	Initial condition for forward amplified spontaneous emission at z=0.
ASE_b*(z=L)=0*	Initial condition for backward amplified spontaneous emission at z=L.

A MATLAB program is developed to evaluate the optimum thulium-doped fibre length for each of the two TDFs of fig. 1. Note that in our simulation the feedbacks of ends' reflection are set to zero and it is only applied forward pump configuration. Figure2 and 3 illustrate the theoretical prediction of the output ASE forward power and the residual pump power for TDF_1 and TDF_2, respectively. The launched pump power is equal 27dBm (0.55 W) at case TDF_1 and 31.7dBm (1.5W) at TDF2. We clearly notice that the optimum fibre length of TDF1 is 1.2 m at 1840nm output ASE as shown in fig. 2. In contrast to TDF2, the optimum fibre length is 5m at 1950nm output ASE as illustrated in fig. 3. In our configuration, 1.2m of TDF_1 is a suitable length to obtain short wavelength bands of ASE source which is centred at 1840nm, whereas 8m of TDF_2 is more suitable to access long wavelength bands which is centred at 1950nm.

The next step is to investigate the output power spectra of ASE at short and long wavelength bands. Figure 4 shows the ASE spectrum of TDF_1 at 1.2m

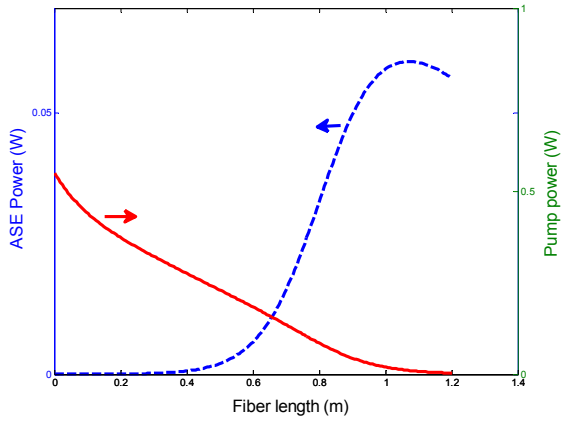

Figure 2: Pump power distribution along TDF_1 length and the forward ASE at 1840nm when the launched pump power is 0.55W.

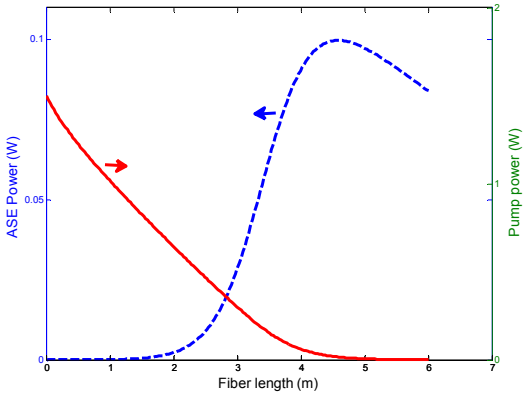

Figure 3: Pump power distribution along TDF_2 length and the forward ASE at 1950nm when the launched pump power is 1.5W.

fibre length and 27dBm launched pump power. The bandwidths of forward ASE has full-width half maximums (FWHM) of approximately 100 nm between 1800nm and 1900nm compared to only 68nm and 88nm in forward and backward ASE obtained by Gorjan et al. (2012). The discrepancies are due to the difference in thulium fibre characteristics. Fig. 5 shows the ASE spectrum of TDF_2 at 8m fibre length and 31.7dBm is the launched pump power. The bandwidth of forward ASE at FWHM is approximately 70 nm between 1900nm and 1970nm. Finally, fig. 6 illustrates the combined ASE spectra of the TDF_1 and TDF_2 spectra. Notes that a wide 50:50 coupler is used and assumed to be flat over the range (1800nm-2000nm). It is clearly seen that the combined ASE provides approximately 170 nm bandwidth at FWHM between 1800nm and 1970nm. Thus, this is the first time to our knowledge that over 170nm bandwidth ASE source based only on thulium-doped fibre is reported.

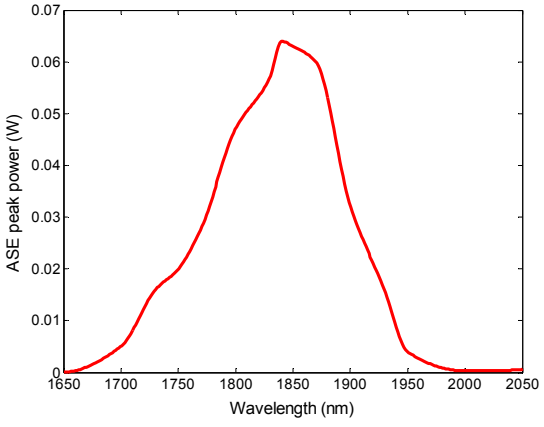

Figure 4: Power spectrum of the forward ASE at 1.2m of TDF_1 when 27dBm is the total input pump power.

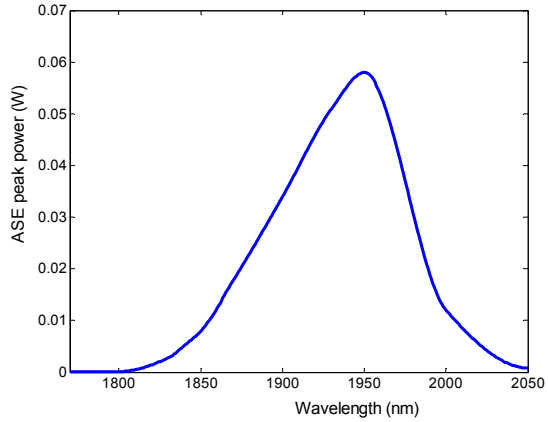

Figure 5: Power spectrum of the forward ASE at 8m of TDF_2 when 31.7dBm is the total input pump power.

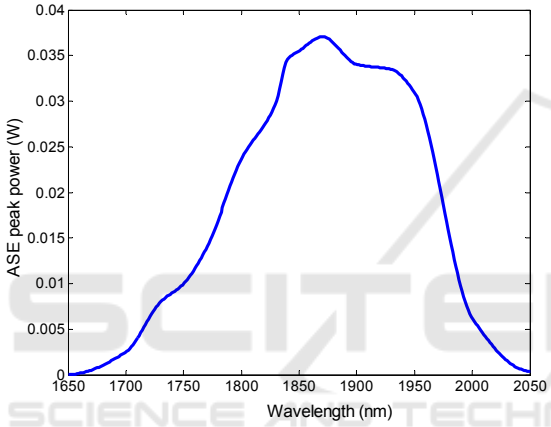

Figure 6: Combined power spectrum of the TDF_1 and TDF_2 ASE spectra by using flat wide 50:50 coupler.

4 CONCLUSION

A theoretical model of ASE generation around 2µm is built up by solving a set of rate and propagation equations. A MATLAB program is developed using the Runge-Kutta method to investigate the behaviour of the ASE generation at 2µm from two different thulium fibres types at 1570nm.

We chose two different fibre characteristics with optimised fibre length in order to generate ASE source for short and long wavelength bands. Wide band ASE source can be generated by combining the two wavelength bands. Thus, the main scope of this study is to generate broad band ASE source at 2 µm for applications that require broader ASE bandwidth such as optical coherence tomography.

Our simulation results show that short wavelength bands (1800nm-1900nm) with 100nm FWHM bandwidth can be generated from the TDF_1. In contrast to long wavelength bands (1900nm-1970nm) with 70nm FWHM bandwidth can be generated from TDF_2. More than 170nm (1800nm-1970nm) should be produced from combining the two above ASE spectra. Note that we choose couplers and combiners have flatting coupling response over the wavelengths range in order to allow broadband ASE source. Hence, our suggested configuration is a suitable arrangement to obtain over 170nm wider broadband source at 2 µm from thulium doped fibre.

REFERENCES

Hu, Z. et al. (2014). 'High power single stage thulium doped superfluorescent fibre source', *Appl. Phys. B.,* 118(1), pp. 101-107.

Li, J. (2014). 'Wide wavelength selectable all-fibre thulium doped fibre laser between 1925 nm and 2200 nm', *Opt. Express,* 22(5), pp. 5387-5399.

Hsu, Z. C. et al. (2008). 'High power broadband all fibre super-fluorescent source with linear polarization and near diffraction-limited beam quality', *Proc. SPIE 7004*, 70044M .

Morse, T. F., Oh, K. and Reinhart, L. J. (1995). 'Carbon dioxide detection using a co-doped Tm-Ho optical fiber', *Proc. SPIE*, 2510, pp.158-164.

Jackson, S. D., Sabella, A. and Lancaster, D. G. (2007). 'Application and development of high-power and highly efficient silica-based fiber lasers operating at 2µm', *IEEE J. Sel. Top. Quantum Electron,* 13(3), pp. 567-572.

Sugimoto, N., Sims, N. Chan, K. and Killinger, D. K. (1990). 'Eye-safe 2.1 μm Ho lidar for measuring atmospheric density profiles', *Opt. Lett.,* 15, pp. 302-304.

Halder, A. et al (2012). 'Wideband Spectrum-Sliced ASE Source Operating at 1900-nm Region Based on a Double-Clad Ytterbium-Sensitized Thulium-Doped Fiber', *IEEE Photonics* J., 4(1), pp. 14-18.

Cheung, C. S. et al. (2015), 'High resolution Fourier domain optical coherence tomography in the 2 µm wavelength range using a broadband supercontinuum source', *Opt. Express*, 23(3), pp. 1992-2001.

Oh, K. et al. (1994). 'Broadband superfluorescent emission of the $^3H_4$ - $^3H_6$ transition in a Tm-doped multicomponent silicate fiber', *Opt. Lett*., 19, pp. 1131-1133.

Shen, D. Y. et al. (2008). 'Broadband Tm-doped superfluorescent fiber source with 11 W single-ended output power', *Opt. Express,* 16(15), pp. 11021-11026.

Tsang, Y., El-Sherif, H. A., and King, T. A. (2005). 'Broadband amplified spontaneous emission fiber source near 2µm using resonant in-band pumping', *J. Mod. Opt.* 52, pp. 109-118.

Gorjan, M., North T. and Rochette, M. 2012. Model of

the amplified spontaneous emission generation in thulium-doped silica fibers, *J. Opt. Soc. Am. B*., 29, 2886.

Yu, G. et al. (2010). 'A theoretical model of thulium-doped silica fiber's ASE in the 1900 nm waveband', *Optoelectron. Lett*. 6(1), 45-47.

Agger, S. D. & Povlsen, J. H. (2006). 'Emission and absorption cross section of thulium doped silica fibers', *Optics express*, 14(1), pp. 50-57.

Jackson, S. D. (2009). 'The spectroscopic and energy transfer characteristics of the rare earth ions used for silicate glass fibre lasers operating in the shortwave infrared', *Laser Photon. Rev*., 3(5), pp. 466–482.

Li, Z. et al. (2013). 'Diode-pumped wideband thulium-doped fiber amplifiers for optical communications in the 1800 – 2050 nm window', *Optics Express*, 21(22), pp. 26450-26455.

Stevens, G., Legg, T. & Way, B. (2015). 'All-fibre widely tunable thulium laser', *Proc. SPIE 9728, Fiber Laser XIII*, 972814.

Jackson, S. D. and King, T. A. (1999). 'Theoretical modeling of Tm-doped silica fiber lasers', *Journal of Lightwave Technology*, 17(5), pp. 948-956.

Whitley T. J. and Wyatt R. (1993). 'Alternative Gaussian spot size polynomial for use with doped fiber amplifiers', *IEEE Photon. Technol. Lett.* 5(11), pp. 1325-1327.

Emami, S. D. (2011). 'Thulium-Doped Fiber Amplifier, Numerical and Experimental Approach', Nova Science Publishers, Inc.